Long Noncoding RNA SNHG16 Functions as Tumor Activator by Sponging hsa-miR-373-3p to Regulate TGFBR2/SMAD Pathway in Prostate Cancer

WuBin Weng
ming dong hospital affiliated to fujian medical university https://orcid.org/0000-0001-8610-078X
ChangMing Liu (Mdyylcm@163.com)
ming dong hospital affiliated to fujian medical university
GuoMin Li
ming dong hospital affiliated to fujian medical university
QiongFang Ruan
ming dong hospital affiliated to fujian medical university
HuiZhang Li
ming dong hospital affiliated to fujian medical university
NingFeng Lin
ming dong hospital affiliated to fujian medical university
GuangBing Chen
ming dong hospital affiliated to fujian medical university

Primary research

Keywords: prostate cancer, lncRNA SNHG16, hsa-miR-373-3p, TGFBR2/SMAD pathway, DU-145 cell

Posted Date: November 17th, 2020

DOI: https://doi.org/10.21203/rs.3.rs-105331/v1

Abstract

Background: Long noncoding RNAs (lncRNAs) are one of the major causes of tumorigenesis. However, the roles and mechanisms of lncRNA SNHG16 in prostate cancer (PCa) remain unknown. The purpose of this study was to elucidate the mechanisms of lncRNA SNHG16 in the proliferation and metastasis of human PCa cells.

Material and Methods: First, the quantitative polymerase chain reaction (qPCR) was used to measure SNHG16 expression in PCa tissues and adjacent normal tissues (n=80). Down-regulate and over-express SNHG16 in human PCa DU-145 cell. Then cell proliferation was detected by CCK8 assay, cell apoptosis was analyzed by flow cytometry, cell migration were determined by wound healing, and cell invasion was examined by transwell. Western blot assays were used to examine the expression of the TGFBR2, c-MYC, E2F4, SMAD2, p-SMAD2, SMAD3, and p-SMAD3. Second, the targeting relationship between SNHG16 and hsa-miR-373-3p was verified by dual-luciferase reporter assay and rescue experiments. Third, the targeting relationship between hsa-miR-373-3p and TGFBR2 was verified by dual-luciferase reporter assay and rescue experiments.

Results: The expression of SNHG16 was significant increase in PCa tissues (Z=-8.405, P<0.001), and with significant correlation with patient's age (<60 and ≥60 years old, P=0.007). Silencing SNHG16 inhibited DU-145 cell proliferation, migration, and invasion, while induced cell apoptosis significantly (P<0.01, respectively). Overexpressing SNHG16 promoted cell proliferation, migration and invasion, and reduced cell apoptosis rate (P<0.05, respectively). SNHG16 overexpression observably increased TGFBR2, c-MYC, E2F4, p-SMAD2, and p-SMAD3 expression (P<0.001, respectively), but SNHG16 inhibition was opposite. However, SNHG16 did not regulate SMAD2 and SMAD3 expression. Next, hsa-miR-373-3p was found down-regulated in PCa tissues (Z=-8.344, P<0.001), and the down-regulation of hsa-miR-373-3p were closely linked to Gleason score (Gleason score: <7 and >7, P = 0.024). Hsa-miR-373-3p expression of hsa-miR-373-3p was negatively correlated with SNHG16 (r=-0.544, P<0.001). The result of dual-luciferase reporter assay and qPCR test revealed that hsa-miR-373-3p was a target of SNHG16. Hsa-mir-373-3p inhibitor could rescue sh-SNHG16-inhibited cell proliferation, migration and invasion by promoting TGFBR2, C-MYC, E2F4, P-Smad2, and P-smad3 expression. Finally, we found that TGFBR2 may be the target gene of hsa-mir-373-3p through TargetScan and starbase. Further research found that TGFBR2 was markedly up-regulated in PCa tissues (Z=-5.945, P<0.001), and the expression of TGFBR2 was negatively correlated with hsa-miR-373-3p (r=-0.627, P<0.001). Dual-luciferase reporter assay and qPCR test showed that TGFBR2 was a target of hsa-miR-373-3p. TGFBR2 knockdown could inhibit hsa-mir-373-3p inhibitor-induced cell proliferation, migration and invasion, and reversed the effect of hsa-mir-373-3p inhibitor on cell apoptosis. Based on the data, sh-TGFBR2 partially disabled hsa-mir-373-3p inhibitor effect.

Conclusion: LncRNA SNHG16 might act as a ceRNA to regulate the proliferation and migration of DU-145 cells by modulating the hsa-miR-373-3p/TGFBR2/SMAD axis.

Background

Incident cases of prostate cancer (PCa) increased 3.7-fold from 1990 to 2015 [1]. The incidence and burden of PCa are steadily increasing globally. Although there were many treatments for prostate cancer patients, such as such as surgery, radiotherapy, androgen deprivation, chemotherapy, bone-targeting agent etc., it remains the third-leading cause of cancer death in men [2]. Because with the development of genome changes and disease severity, molecular complexity was increased, which affect PCa metastasis, clinical relevance and precision therapy [3]. Hence, carcinogenesis and intrinsic mechanism associated with the tumorigenesis of PCa should be further explored to provide a promising method for detection and intervention.

Studies have proved that non-coding RNA plays a role in the occurrence, progression and treatment of PCa. For example, long noncoding RNAs (lncRNAs) with > 200 bases in length and transcribed from the genomic intergenic regions, which regulated the expression of genes at epigenetic, transcriptional and post-transcriptional levels. LINC00844 regulated global androgen receptor-regulated genes in PCa by facilitating androgen receptor binding to chromatin, and inhibited the progression and metastasis of PCa by activating the expression of the important cancer metastasis suppressor NDRG1 [4]. LncRNA HOXD-AS1 recruited WDR5 to directly regulate the expression of target genes by mediating histone H3 lysine 4 tri-methylation, thus promoting PCa proliferation, castration resistance, and chemo-resistance [5]. LncRNA PCA3 promoted PCa cell growth by down-regulated the tumor suppressor gene PRUNE2 [6]. LncRNA can act as a tumor activator or inhibitor in PCa.

Importantly, LncRNA acts as a competitive endogenous RNA (ceRNA) to regulate MicroRNAs (miRNAs) expression is one of the important mechanisms of its post-transcriptional regulation. MiRNAs are a type of small non-coding RNA with length of 17–22 nucleotides. The production of miRNAs is based on the action of Dicer, which is a kind of RNase that processes the hairpin structured precursors into mature miRNA. Then, the transcribed miRNA suppresses gene expression by recognizing the complementary target site in the 3'untranslated region (UTR) of the target mRNAs [7]. MiRNAs can serve as oncomiRs by targeting tumor suppressor genes and as tumor suppressor by targeting oncogenes, and miRNA-targeted therapeutics have development [8]. LncRNA function as ceRNA by competitively occupying the shared binding sequence of miRNAs, thereby isolating miRNAs and changing the expression of their downstream target genes. Based on the relationship between lncRNAs and miRNAs and mRNAs, He JH et al. screened out 19,075 regulatory relationships which might be involved in the pathogenesis of PCa [9]. The function abnormalities of lncRNA-miRNA-mRNA regulatory network are closely related to the occurrence and development of PCa.

LncRNA small-nucleolar RNA host gene 16 (SNHG16) was a novel tumor oncogene identified in many cancers. SNHG16 was found to be overexpressed in PCa patients, which promoted GLUT-1 expression to induce glucose uptake and PCa cell proliferation [10]. In cervical cancer, SNHG16 promoted tumor progression by directly targeted miR-216A-5p/ZEB1 axis [11]. In hepatocellular carcinoma, SNHG16 accelerated tumor development via regulating expression of miR-17-5p/p62 axis and activating mTOR

and NF-κB pathways [12]. Bsides, SNHG16 acted as a ceRNA to drive vascular endothelial cells proliferation, Vasoformation, migration, and invasion through modulating miR-520d-3p/STAT3 axis [13]. A research revealed that miR-373-3p decreased might increase PCa cell invasion via activating TGFBR2/p-Smad3 signals [14]. We analyzed TargetScan and starbase, and found that there were binding site between SNHG16 and hsa-miR-373-3p, hsa-miR-373-3p and TGFBR2. Because of the regulation between SNHG16 and hsa-miR-373-3p in PCa is still unclear, and the complex role of TGFBR2 [15, 50]. This study intends to analyze the relationship between SNHG16, hsa-miR-373-3p and TGFBR2 to explore its potential mechanism of effect on PCa.

Materials And Methods

Clinical Tissues Collection

Eighty PCa patients at the Mindong Hospital Affiliated to Fujian Medical University, between Feb 2019 and Jan 2020, were enrolled into the study. The PCa tumor and adjacent normal tissues samples were collected. All patients were confirmed as PCa by histopathological analysis and without preoperative radiotherapy or chemotherapy. All fresh specimens were stored in liquid nitrogen immediately at −80 °C until use. The detailed criteria for the patients were that the pathological type is adenocarcinoma. The clinical parameters of the enrolled patients such as age, TNM stage and Gleason score et al were recorded and analyzed to correlate the in vitro findings with the clinical presentations (Table 1). All patients signed the relevant informed consent. The Ethics Committee of Mindong Hospital Affiliated to Fujian Medical University approved the study protocol. The batch number was [2019] NingMin Medical Ethics No (0110-1). The investigation adhered to the principles outlined in the Declaration of Helsinki.

RNA extraction and qRT-PCR

Total RNA was extracted from PCa tissue and cells by NucleoZOL® (Gene Co., Ltd., Shanghai, China). Primers were resuspended by adding 250 μL of RNase-free water. Master mix was prepared for each mRNA-specific assay. Each single reaction included 10 μL of qPCR SYBR® Green Master Mix Universal (Takara Bio, Inc., Japan). About 10 μL of the primer was set for an individual miRNA. RNase free water (3 μL) and RT product (2 μL) were added to a single real-time PCR reaction tube as template.

Reverse transcription (RT) was performed using the RT System Kit (Takara Bio Inc., Tokyo, Japan). The synthesized cDNA was amplified by quantitative PCR by using HEAL FORCE (Xianggang, China). The reaction conditions included 42 °C for 60 min, followed by cooling to 4 °C. The resultant cDNA was used as template for subsequent PCR. Forty PCR amplification cycles were performed with initial incubation at 95 °C for 10 min and final extension at 72 °C for 5 min. Each cycle comprised denaturation at 95 °C for 10 s, annealing at 60 °C for 30 s, and extension at 72 °C for 30 s. The GAPDH mRNA was a control. The relative expression of candidate genes was calculated using the formula $\Delta\Delta Cq = (C_{q,\,target} - C_{q,\,reference})_{PCa} - (C_{q,\,target} - C_{q,\,reference})_{NC}$, and the estimated expression ratio was equal to $2^{-\Delta\Delta Cq}$ [16]. The estimated expression ratio was equal to $2^{-\Delta\Delta Cq}$. The primer set of candidate gens: LncRNA SNHG16 FORWARD

primer was GTGCCTCAGGAAGTCTTGCC; REVERSE primer was ATCCAAACAAGTTATCAGCAGCAGCAC. TGFBR2 FORWARD primer was GTAGCTCTGATGAGTGCAATGAC; REVERSE primer was CAGATATGGCAACTCCCA GTG. GAPDH FORWARD primer was ATGGGGAAGTGAAGGTCG; REVERSE primer was TTACTCCTTGGAGCCATGTG.

Taqman RT- PCR

The RNA harvested from PCa tissue and cells was extracted by the miRNeasy mini kit (Qiagen, USA). Before RNA extraction, each sample was added with 100 ng exogenous and synthetic Caenorhabditis elegans miR-39 to normalize. Specifically, sample suspension (50 mg tissue) was mixed with Qiazol lysis reagent (1 mL), incubated or homogenate for 5 min in room temperature, and then mixed with 200 µL cholorform for 3 min. The RNA was separated at 12,000×g for 15 min at 4°C and collected the aqueous phase. After centrifugal, the supernatant mixed with 100 % ethanol (600 µL). In order to purify RNA, 700 µL supernatant was added to miRNeasy mini spin column and centrifuged at 8,000 × g for 15s at room temperature. Then, miRNA was eluted by the addition of 30 µl RNase-free water. Concentration of RNA was measured by nanodrop.

To confirm hsa-mir-373-3p expression, the Taqman real-time PCR was used (Applied Biosystems, Foster City, CA, USA). 5 µL RNA was reversely transcribed into cDNA using the Taqman miRNA reverse transcription kit (Applied Biosystems, USA). The reaction conditions were 16 °C for 30 min, 42 °C for 30 min, and 85 °C for 5 min. Then, 10 µL of TaqMan® Universal PCR Master Mix (Applied Biosystems, USA), 1 µL of TaqMan Stem-loop miRNAassay, 7.5 µL of nuclease free water, and 1.5 µL of RT product were used for real-time PCR reaction. Forty cycles of PCR amplification were performed, with initial incubation at 95 °C for 10 min. Each cycle comprised at 95 °C for 15 s and annealing at 60 °C for 1 min. The stem-loop primers were 5 nM each: cel-miR-39: GTCGTATCCAGTGCAGGG TCCGAG-GTATTCGCACTGGATACACCAAGCT, hsa-miR-373-3p: GTCGT ATCCAGTG CAGGGTCCGAGGTATTCGCACTGGATACGACCTTCAC. The estimated expression ratio of hsa-miR-373-3p was equal to $2^{-\Delta\Delta Cq}$.

Cell culture and transfection

Human PCa DU-145 cell line was purchased from the American Type Culture Collection (Manassas, VA, USA). Cells were grown in RPMI-1640 medium (Gibco, USA) and cultured in the media with 10% FBS (PAN biotech, Germany), 4 mM L-glutamine, 100 U/mL penicillin, and 100 µg/mL streptomycin. The cells were incubated at 37 °C in a humidified atmosphere of 5% CO_2.

1×10^5 cells/well of DU-145 cell was inoculated into 24-well plates before transfection. Lipofectamine 2000 (Invitrogen, USA) was utilized for cell transfection. For SNHG16 gene knockdown experiment, shRNA was amplified by the following primers, then the product was digested with *BamHI* and *EcoRI* restriction enzymes (Fermentas, UK), and the fragment was inserted into the *BamhI/EcoRI* sites of the pLVX-shRNA2-Puro vector. The shRNA targeting SNHG16 was 5'-GATCCGGATGAGACTTAACTTAAATTCAAGAGATTTAAGTTAA GTCTCATCCTTTTT G-3', negative control

shRNA was 5'-GATCCG TGTAGATGCGTTGTGATATTCAAGAGAT ATCACAACGCATCTACACTTTTTG-3' (Life Technologies, Carlsbad, CA, USA). For SNHG16 overexpression, the cells were transfected with the SNHG16 overexpression construct (pcDNA3.1-SNHG16). Specifically, the full-length of SNHG16 was obtained via PCR amplification using the primers: SNHG16-F: 5'-CGGGATCCCGGCGTTCTTTTCGAGGTCGGCCG-3' and SNHG16-R: 5'-CCCTCGAGGGTGACGGTAGTTTCCCAAGTTTA-3'. Then, the amplification the product was digested with *BamhI* and *XhoI* restriction enzymes, and the fragment was inserted into the *BamhI/XhoI* sites of the PcDNA3.1 vector (Invitrogen; Thermo Fisher Scientific, Inc., USA) to obtain a SNHG16 overexpression plasmid. Hsa-miR-373-3p mimics, inhibitors and negative control were purchased from GenePharma (Shanghai, China). The shRNA targeting TGFBR2 was 5'- GGTGGGAACTGCAAGATACATCUGUGCUGU CCATGTATCTTGCAGTTCCCACCTTTTT-3', the negative control shRNA was 5'-GATCCGAUCAAUACUAUUCAUCAATTCAAGAGAUUGAUGAAUAGUAUUGAUCTTTTTG-3'. The pLVX-shRNA2-Puro vector, *EcoRI* and *BamhI* were used to construct TGFBR2 knockdown and negative control plasmid. When cells grew to 30%–50% confluence, the plasmid (10 nM) was utilized to transfect. After 48 h of transfection, relevant tests were used for comparison.

CCK-8 assay for cell proliferation

The transfection cells were determined by Cell Counting Kit-8 assay (Dojindo, Japan). DU-145 cell suspensions (1×10^4/mL) were transferred to 96-well plates and incubated for 24, 48, 72, and 96 h. Each well was added with 10 μL of CCK-8 and incubated for 4 h. The values of each well were measured by a microplate reader (PERLONG, Beijing, Chia) at 450 nm. All experiments were repeated three times.

Flow cytometric analysis for cell apoptosis

The 1×10^5 cells/ well were cultured in 24-well plates and transfected until the confluence reached 60%–70%. After transfecting with plasmid for 48 h, the cells were washed two times with PBS and centrifuged for 5 min at 1000 rpm. According to the instruction, the cells were then incubated with 5 μL of Annexin V-FITC for 15 min and 10 μL of PI for 5min at room temperature and dark (BD Biosciences, USA). Finally, the cells were detected by flow cytometry (Becton Dickinson, USA). All experiments were repeated three times.

Wound healing assay for cell migration

Wound healing test was used to measure cell migration. After transfecting with plasmid for 48 h cells were reaped. A total of 3×10^5 cell/well were inoculated into 24-well plates, which each well has cell plug-in. Wound healing experiment was carried out when all the cells were adherent and just full. After incubation for 24 h, the cells were counted under the microscope. All experiments were repeated three times.

Transwell assay for cell invasion

Cell invasion was assayed using a Transwell chamber (8 μm pore size, Corning) deposited with Matrigel (BD Biosciences, USA). After transfecting with plasmid for 48 h, 1×10^5 cell/well was inoculated into Transwell's upper chamber. The lower chamber was added with complete media. After 24 h, cells that remained in the upper membrane were removed. The migrated cells were incubated with 4% paraformaldehyde for 30 min, stained with 0.1% crystal violet for 15 min, and counted in the microscope. All experiments were repeated three times.

Western blot

After transfecting 48 h, DU-145 cells were collected. RIPA buffer (Takara Bio Inc., Tokyo Japan) and protease inhibitor (Roche Diagnostics) were used for cell lysis. BCA assay kit was used to detect protein concentration (Epizyme, China). The protein samples were separated using SDS–PAGE and shifted to PVDF. The PVDF membranes were saturated with blocking buffer (5% skim milk in 20 mM Tris–HCl, 150 mM NaCl, 0.1% Tween-20) for 1 h at room temperature and incubated with primary antibodies (1:1000) at 4 °C overnight. The antibodies of TGFBR2, c-MYC, E2F4, SMAD2, p-SMAD2, SMAD3, p-SMAD3, and β-actin (Cell Signaling Technology, Beverly, MA, USA) were used. After washing two times with PBS, the cells were incubated with secondary-HRP-antibodies (Protein-Tech, USA) for 2 h at room temperature. The membranes were added with ECL Western blotting reagents (GE Healthcare, USA) to detect protein levels. The bands were imaged by Tanon 5200 Biotanon. Image J software was used to calculate the gray value.

Double-luciferase reporter assay

SNHG16-3'-UTR-wild-type (WT) sequence was gag tttcagagag taatgcttaa ccccagttac acaggatgcc gtcttgtgtt tcctcttgtt tagttaccca ctacagtgat tttgtgatct gctaatgggt tgccacccac aaccattgct ttaACGCTTt tacttcaaat caatgaagga ttgataaaag ttctcctggt gtctccgcag agtgccttcc aggaacagat ctttgcatag aatatcagtg gtttccttt ttgtttcaaa tagtggtcaga. SNHG16-3'-UTR-mutant (MUT) sequence was gag tttcagagag taatgcttaa ccccagttac acaggatgcc gtcttgtgtt tcctcttgtt tagttaccca ctacagtgat tttgtgatct gctaatgggt tgccacccac aaccattgct ttagcacttt tacttcaaat caatgaagga ttgataaaag ttctcctggt gtctccgcag agtgccttcc aggaacagat ctttgcatag aatatcagtg gtttccttt ttgtttcaaa tagtggtcaga. TGFBR2 3'-UTR -WT sequence was ggaataaca ttctgtagtt cctaaaaata ctgacttttt tcactactat acataaaggg aaagttttat tcttttatgg aacacttcag ctgtactcat gtattaaaat aggaatgtga atgctatata ctctttttat atcaaaagtc tcaagcactt atttttattc tatgcattgt ttgtctttta cataaataaa atgtttatta gattgaataa agcaaaatac tcaggtgagc atcctgcctc ctgttcccat tcctagtagct. Then, THBS1 3'-UTR- MUT sequence was ggaataaca ttctgtagtt cctaaaaata ctgacttttt tcactactat acataaaggg aaagttttat tcttttatgg aacacttcag ctgtactcat gtattaaaat aggaatgtga atgctatata ctctttttat atcaaaagtc tcaCAGAtCt atttttattc tatgcattgt ttgtctttta cataaataaa atgtttatta gattgaataa agcaaaatac tcaggtgagc atcctgcctc ctgttcccat tcctagtagct. These sequences were synthesized (GenePharma, Shanghai, China) and digested with *XhoI* and *NotI* restriction enzymes (Fermentas, UK). Then, the 3'-UTR fragment was inserted into the *XhoI/NotI* sites of the psiCHECK-2 vector (Promega, USA) to obtain luciferase reporter plasmid.

DU-145 cell suspensions (1×10^5 cell/well) were transferred to 24-well plates and incubated for 24 h. In order to verify the targeting effect of SNHG16 and hsa-miR-373-3p, the psiCHECK-2-SNHG16-WT or psiCHECK-2-SNHG16-MUT reporter plasmids (20 ng) were cotransfected with hsa-miR-373-3p mimic or mimic negative control (10 nM) into cells by using Lipofectamine 2000 (Invitrogen, USA). When verifying the targeting effect of TGFBR2 and hsa-miR-373-3p, the psiCHECK-2-TGFBR2-WT or psiCHECK-2-TGFBR2-MUT reporter plasmids (20 ng) were cotransfected with hsa-miR-373-3p mimic or mimic negative control (10 nM) into cells by using Lipofectamine 2000. After 36 h of transfection, cell lysates were prepared by using lysis buffer (Promega, Madison, USA). The firefly and Renilla luciferase activities were detected according to dual luciferase reporter assay (Promega, Madison, USA). The Renilla luciferase values were then divided by the firefly luciferase activity values to normalize the difference in transfection efficiency. All experiments were repeated three times.

Statistical analysis

All experiments were analyzed by the IBM SPSS Statistics 20.0 software (IBM Corp., Armonk, New York, USA). If data followed normal distribution, the one-way ANOVA analysis with LSD post-hoc test was performed. If the data did not follow normal distribution, Mann–Whitney U test was used. Spearman correlation was used to analyze the correlation between SNHG16 and hsa-mir-373-3p, hsa-mir-373-3p and TGFBR2. Chi-square test was used to descriptive analysis. Datas were presented as mean ± standard deviation, and $P < 0.05$ indicated significant difference.

Results

The correlation with patient's characteristics and SNHG16, hsa-miR-373-3p and TGFBR2 expression

Division of the 80 patients into those with high expression of SNHG16, hsa-miR-373-3p and TGFBR2, and those with low expression was done using the difference value to assess the link between the molecule and the clinical characteristics (Table 2). First, we analyzed the expression of SNHG16, hsa-miR-373-3p and TGFBR2 in PCa according to the patient's age (age groups: <60, 60≥years old). SNHG16 expression was higher in patient's age ≥60 years old (P=0.007), whereas in these two groups of patients (<60 and 60≥ years old) hsa-miR-373-3p and TGFBR2 expression lost its significance (P=0.789, P=0.606, respectively). Second, the expression of SNHG16, hsa-miR-373-3p and TGFBR2 were analyzed according to the Gleason score (Gleason score: <7, >7). The up-regulation of SNHG16 and TGFBR2 in PCa patients were no statistical correlation with Gleason score (All $P > 0.05$). However, the down-regulation of hsa-miR-373-3p were closely linked to Gleason score ($P = 0.024$). Third, SNHG16, hsa-miR-373-3p and TGFBR2 expression were analyzed according to the TNM stage (TNM stage: T1, T2, T3/4). The results showed that there were no significant correlation with gene expression and TNM stage (All $P > 0.05$).

The high expression of SNHG16 in PCa tissues promoted tumor cell proliferation, migration and invasion by regulating TGFBR2/SMAD signaling

The result of qRT-PCR showed SNHG16 was significantly increased in PCa tissues comparison with adjacent normal tissues (P<0.001) (Fig. 1A). SNHG16 might play an important role in tumor progression [10]. In order to study the role of SNHG16 in PCa, we knocked down and overexpressed SNHG16 in DU-145 cells (Fig. 1B). Then, we further explored the biological role of SNHG16 in DU-145 cell. SNHG16 knockdown significantly suppressed cell proliferation (P<0.001), and SNHG16 overexpression significantly promoted cell proliferation (P<0.001) (Fig. 1C). Knockdown of SNHG16 significantly increased cell apoptosis (P<0.001), and the overexpression of SNHG16 significantly inhibited cell apoptosis (P<0.01) (Fig. 1D). The transwell test revealed that inhibition of SNHG16 expression significantly reduced cell invasion (P<0.01), and up-regulation of SNHG16 expression notably increased the number of cell invasion (P<0.05) (Fig. 1E). The wound healing test showed SNHG16 inhibition significantly decreased cell migration (P<0.001), and SNHG16 up-regulation markedly increased the number of cell migration (P<0.001) (Fig. 1F).

Next, the protein expression levels of c-MYC, TGFBR2, E2F4, SMAD2, p-SMAD2, SMAD3, and p-SMAD3 were determined by Western blot. The protein expression levels of c-MYC, TGFBR2, p-SMAD2, p-SMAD3, and E2F4 significantly decreased in the sh-SNHG16 group compared with those in the sh-NC group (P<0.001), but these proteins were significantly increased in the OE-SNHG16 group compared with those in the OE-NC group (P<0.001) (Fig. 1G). However, the SMAD2 and SMAD3 expression were not affected by SNHG16 (Fig. 1G). Our results indicated that the part effect of SNHG16 promoted cell proliferation, migration and invasion via activating the TGFBR2/SMAD signaling pathway.

SNHG16 acts as miR-373-3p sponge to affect DU-145 cell biological processes via regulating TGFBR2/SMAD signaling

The analysis of TargetScan and starbase showed that there is a binding site between SNHG16 and hsa-miR-373-3p (Fig. 2A). To study the effect between SNHG16 and miR-373-3p, the qRT-PCR was used to detect hsa-miR-373-3p expression and revealed it was significantly decreased in PCa tissues comparison with adjacent normal tissues (P<0.001) (Fig. 2B). Spearman correlation analysis revealed the expression of hsa-miR-373-3p had negative correlations with SNHG16 (r = -0.544, P< 0.001) (Fig. 2C). Then, the DU-145 cells were transfected hsa-miR-373-3p mimic and inhibitor (Fig. 2D). The bioinformatical prediction was verified by dual-luciferase reporter experiment. Compared to the miR-NC (negative control), hsa-miR-373-3p mimic significantly suppressed the luciferase activity of psiCHECK-2-SNHG16-WT, while did not affect the luciferase activity of psiCHECK-2-SNHG16-MUT (Fig. 2E). Besides, SNHG16 knockdown was significantly up-regulated hsa-miR-373-3p expression, while the hsa-miR-373-3p inhibitor partially reversed this trend (Fig. 2F). This indicated that SNHG16 directly interacted with hsa-miR-373-3p at the predicted binding site.

Next, a rescue assay was conducted to check the involvement of hsa-miR-373-3p in the role played by SNHG16 on the growth of tumor. First, we detected the capability of proliferation, apoptosis, migration and invasion of DU-145 cells transfected with hsa-miR-373-3p inhibitor or/and sh-SNHG16. Inhibition of hsa-miR-373-3p significantly promoted cell proliferation (P<0.001), and hsa-miR-373-3p inhibitor reversed

the suppression of SNHG16 depletion on cell proliferation (P<0.001) (Fig. 2G). Knockdown of hsa-miR-373-3p significantly decreased cell apoptosis (P<0.05), and hsa-miR-373-3p inhibitor reversed the facilitation of SNHG16 depletion on apoptosis (P<0.01) (Fig. 2H). The transwell test revealed that inhibition of hsa-miR-373-3p expression significantly induced cell invasion (P<0.05), and hsa-miR-373-3p inhibitor reversed the suppression of SNHG16 depletion on cell invasion (P<0.01) (Fig. 2I). The wound healing test showed hsa-miR-373-3p reduction significantly increased cell migration (P<0.05), and hsa-miR-373-3p inhibitor reversed the suppression of SNHG16 depletion on cell migration (P<0.01) (Fig. 2J).

Furthemore, the protein expression levels of c-MYC, TGFBR2, E2F4, SMAD2, p-SMAD2, SMAD3, and p-SMAD3 were determined by Western blot. Compared with the NC group, the protein expression levels of c-MYC, TGFBR2, p-SMAD2, p-SMAD3, and E2F4 significantly increased in the hsa-miR-373-3p inhibitor group (P<0.05, respectively). The expression of c-MYC and E2F4 were significantly increased and TGFBR2 expression was decreased observably when co-transfected with hsa-miR-373-3p inhibitor and sh-SNHG16 (P<0.05). Besides, hsa-miR-373-3p inhibitor reversed the suppression of SNHG16 depletion on c-MYC, TGFBR2, p-SMAD2, p-SMAD3, and E2F4 protein expression (P<0.05) (Fig. 2K). However, the SMAD2 and SMAD3 expression were not affected by hsa-miR-373-3p inhibitor (Fig. 2K). Our results indicated that inhibition hsa-miR-373-3p partially reversed the suppression of SNHG16 knockdown on cell proliferation, migration and invasion by activating the TGFBR2/SMAD signaling pathway.

Hsa-miR-373-3p target TGFBR2 to mediate DU-145 cell biological processes

The analysis of TargetScan and starbase showed that there is a binding site between hsa-miR-373-3p and TGFBR2 (Fig. 3A). The result of qRT-PCR showed that TGFBR2 mRNA was significantly increased in PCa tissues comparison with adjacent normal tissues (P<0.001) (Fig. 3B). Spearman correlation analysis revealed the expression of TGFBR2 had negative correlations with hsa-miR-373-3p (r = -0.627, P< 0.001) (Fig. 3C). Then, the bioinformatical prediction was verified by dual-luciferase reporter experiment. Compared to the miR-NC (negative control), hsa-miR-373-3p mimic significantly suppressed the luciferase activity of psiCHECK-2-TGFBR2-WT (P<0.01), while did not affect the luciferase activity of psiCHECK-2-TGFBR2-MUT (Fig. 3D). Besides, hsa-miR-373-3p mimic was significantly down-regulated TGFBR2 mRNA expression, while the hsa-miR-373-3p inhibitor markedly up-regulated TGFBR2 mRNA expression (P<0.001) (Fig. 3E). This indicated that hsa-miR-373-3p directly interacted with TGFBR2 at the predicted binding site [14].

Next, a rescue assay was conducted to check the involvement of TGFBR2 in the role played by hsa-miR-373-3p on the growth of tumor. First, we detected the capability of proliferation, apoptosis, migration and invasion of DU-145 cells transfected with hsa-miR-373-3p inhibitor or/and sh-TGFBR2. Down-regulation of TGFBR2 significantly inhibited cell proliferation (P<0.001), and TGFBR2 knockdown reversed the facilitation of hsa-miR-373-3p inhibitor on cell proliferation (P<0.001) (Fig. 3F). Knockdown of TGFBR2 significantly induced cell apoptosis (P<0.001), and TGFBR2 down-regulated reversed the inhibition of hsa-miR-373-3p inhibitor on apoptosis (P<0.001) (Fig. 3G). The transwell test revealed that depletion of TGFBR2 expression significantly suppressed cell invasion (P<0.001), and interference TGFBR2

expression reversed the promotion of hsa-miR-373-3p inhibitor on cell invasion (P<0.01) (Fig. 3H). The wound healing test showed TGFBR2 reduction significantly decreased cell migration (P<0.001), and TGFBR2 knockdown reversed the acceleration of hsa-miR-373-3p inhibitor on cell migration (P<0.01) (Fig. 3I). TGFBR2 knockdown partially reversed the facilitation of hsa-miR-373-3p inhibitor on cell proliferation, migration and invasion. These results demonstrated that SNHG16 acted as a ceRNA to modulate the miR-373-3p/TGFBR2 axis.

Discussion

PCa is one of the main lethal diseases among the cancer mortality rate of men, and the incidence rate increased significantly than in the past [1, 2]. Therefore, a novel target should be identified to improve the prognostic outcome of patients with PCa for developing effective therapeutic treatments. The functions of lncRNAs in PCa tumorigenesis have received increasing attention. LncRNAs can fold into secondary and tertiary structures and function as modulators of biological processes in most cancer types, including PCa [4–6]. Several lncRNAs, such as LINC00844 [4], HOXD-AS1 [5], PCA3 [6] and SChLAP1 [17] etc., are dysregulation in the tumorigenesis of PCa and play oncogenic or tumor-suppressive roles. Here, a kind of lncRNA SNHG16 was found as a potential oncogene modulates PCa cell biological function via hsa-miR-373-3p /TGFBR2/SMAD signaling axis.

A novel lncRNA SNHG16 of PCa has been originally explored as a tumor activator in neuroblastoma and is located on chromosome 17q25.1. SNHG16 was abnormally expressed in patients with aggressive neuroblastoma and acted like an oncogene [18]. SNHG16 might be a prognostic indicator as a potential tumor target and functional regulator in tumorigenesis. The upregulated expression of SNHG16 significantly associated with invasion depth, lymph node metastasis, TNM stage and histological differentiation of gastric cancer [19]. However, SNHG16 was markedly down-regulated and induced tumor-suppressing effects in hepatocellular carcinoma [20]. SNHG16 in multiple cancer types can be either positively or negatively regulated possibly due to the intrinsic subtypes of specific cancer. In this study, the up-regulation of SNHG16 expression in PCa tissues was significantly related to the patient's age (< 60 and 60 ≥ years old, P = 0.007), and the higher the high expression rate of SNHG16 when the Gleason score > 7 or T3/T4 stage. Older age was associated with the Gleason score ≥ 7 or prostatectomy T3/T4 [21]. Age was an independent predictor of shorter PCa-specific survival patients diagnosed with de novo metastatic PCa [22]. Besides, the overexpresion of SNHG16 would induce PCa cell proliferation, migration and invasion. In consequence, SNHG16 might play the oncogenic effects in PCa development or progression.

Recent research reports, SNHG16 over-expressed in PCa patients and play a role in promoting cell proliferation by regulating GLUT-1 expression and glucose uptake [10]. Here, we found SNHG16-incuded DU-145 cell proliferation, migration and invasion via up-regulating c-MYC, TGFBR2, E2F4, p-SMAD2, and p-SMAD3 expression. The c-MYC is a proto-oncogene and plays a role in cell cycle progression, apoptosis and cellular transformation. The high expression of c-MYC could promote the development of PCa by the transcription of the androgen receptor gene and enhance the stability of the full-length androgen receptor

and androgen receptor splice variants proteins [23]. E2F4 were overexpressed in PCa epithelial cells [24], and regulated cell cycle by forming complexes with P130 [25]. E2F5 overexpression induced uncontrolled cellular proliferation by up-regulating phosphorylation of SMAD3 and p38 in PCa [26]. The endogenous SMAD2/3 interacted with PKCε to cause SMAD3 to bind to the promoter of glycolysis genes, induced the expression of glycolysis genes HIF-1α, HKII, PFKP and MCT4 and promoted aerobic glycolysis, thereby promoting PCa cell proliferation [27]. In addition, overexpression of SMAD3 could also enhance aerobic glycolysis and PCa cell proliferation in an independent manner that activated protein kinase D or TGF-β [27]. However, SMAD3 or TGFBR2 null were significantly reduced the mass and microvascular density of PCa xenograft tumors [28]. Therefore, SNHG16 increased the expression of c-MYC, TGFBR2, E2F4, p-SMAD2, and p-SMAD3, which was an important mechanism for its carcinogenic effects.

Numerous lines of evidence showed that lncRNAs can function as ceRNA by sequestering miRNAs [29]. MiRNAs are single-stranded, noncoding RNAs that regulate gene expression via the mechanisms of conserved across metazoans. In this study, hsa-miR-373-3p was significantly decreased in PCa tissues, and had significantly negative correlations with SNHG16 ($r = -0.544$). In addition, the low expression of hsa-miR-373-3p was significantly related to the Gleason score, and the low expression rate of hsa-miR-373-3p when the T2 or T3/T4 stage increased. Hsa-miR-373-3p might act as a tumor suppressor in PCa. Mechanistically, SNHG16 acted as a tumor promoter by serving as hsa-miR-373-3p sponge and up-regulating the TGFBR2 gene to promote PCa progression. The results of Qiu X et al also revealed that hsa-miR-373-3p could activing TGFBR2/p-Smad3 pathway to reduce PCa cell invasion [14]. In several cancers, hsa-miR-373-3p also exerted a tumor suppressor effect. In breast cancer, hsa-miR-373 restrained tumor progression, metastasis and inflammation of by inhibiting NF-κB and TGF-β/TGFBR2/SMAD pathway [30]. High expression of hsa-miR-373 repressed TGF-β-induced epithelial mesenchymal transition, thereby inhibiting the invasion and peritoneal dissemination of pancreatic cancer cells [31]. However, in testicular germ cell tumors, miR-373 could promote proliferation and tumorigenesis of testicular germ cell by neutralizing p53-mediated CDK inhibition [32]. Hence, hsa-miR-373-3p has a dual function as a promoter or suppressor in different cancers. TGFBR2 was an important cancer driver in gastric cancer and liver tumorigenesis [33, 34]. Besides, the down-regulation of TGFBR2 inhibited the expression of SMAD-dependent metastasis-promoting genes PTHrP, PAI-1 and ANGPTL4, and breast cancer cell invasion [30]. The effects of TGF-β/TGFBR2 signaling in PCa progress was strongly dependent on the stage of development, which acted as a tumor suppressor in early stages and acted as a promoter in later stages [35]. In this study, the high expression of TGFBR2 might be related to the inclusion of more advanced patients.

In conclusion, this study revealed that the high expression of SNHG16 promoted the proliferation, migration and invasion of turomr cell via functionally sponging hsa-miR-373-3p and regulating the TGFBR2/SMAD pathway, especially in patients with advanced PCa. However, this study has several limitations. First, the study only analyzed the association of SNHG16, has-miR-373-3p and TGFBR2 in DU-145 cell line. More than one cell lines should be studied. Second, we did not design the animal model to verify the role of SNHG16. In the future, additional clinical and animal experiments are needed to

demonstrate that SNHG16 act as a ceRNA and regulates the hsa-miR-373-3p /TGFBR2 axis, thereby affecting the biological function of PCa cells.

Conclusions

LncRNA SNHG16 acted as a ceRNA to enhance the proliferation, migration, and invasion of PCa cells by modulating the hsa-miR-373-3p/TGFBR2 axis. These data provide novel insights into SNHG16, which may be a novel target for treatment of PCa.

Declarations

Ethics approval and consent to participate: The Ethics Committee of Mindong Hospital Affiliated to Fujian Medical University approved the study protocol. The batch number was [2019] NingMin Medical Ethics No (0110-1). The investigation adhered to the principles outlined in the Declaration of Helsinki.

Consent for publication: All co-authors consented that the manuscript published in *Cancer Cell International*.

Availability of data and materials: All data analyzed and displayed in the present manuscript are available from the corresponding author upon reasonable request.

Competing interests: The authors declare that they have no competing interest.

Funding: The study was supported by [the Natural Science Foundation of Fujian province] under Grant [Project No: 2018J01220].

Authors' contributions: WuBin Weng and ChangMing Liu made substantial contributions to the conception and design of the work. WuBin Weng, ChangMing Liu, GuoMin Li, QiongFang Ruan, HuiZhang Li, NingFeng Lin and GuangBing Chen made substantial contributions to the acquisition, analysis and interpretation of data for the work. WuBin Weng participated in drafting the work, and ChangMing Liu revising it critically for important intellectual content.

Acknowledgements: We would like to thank all the authors listed for their contribution to the present study.

References

1. Pishgar F, Ebrahimi H, Saeedi Moghaddam S, Fitzmaurice C, Amini E. Global. Regional and National Burden of Prostate Cancer, 1990 to 2015: Results from the Global Burden of Disease Study 2015. J Urol. 2018;199(5):1224–32.
2. Litwin MS, Tan HJ. The Diagnosis and Treatment of Prostate Cancer: A Review. JAMA. 2017;317(24):2532–42.

3. Arora K, Barbieri CE. Molecular Subtypes of Prostate Cancer. Curr Oncol Rep. 2018;20(8):58.
4. Lingadahalli S, Jadhao S, Sung YY, Chen M, Hu L, Chen X, Cheung E. Novel LncRNA LINC00844 Regulates Prostate Cancer Cell Migration and Invasion through AR Signaling. Mol Cancer Res. 2018;16(12):1865–78.
5. Gu P, Chen X, Xie R, Han J, Xie W, Wang B, Dong W, et al. lncRNA HOXD-AS1 Regulates Proliferation and Chemo-Resistance of Castration-Resistant Prostate Cancer via Recruiting WDR5. Mol Ther. 2017;25(8):1959–73.
6. Salameh A, Lee AK, Cardó-Vila M, Nunes DN, Efstathiou E, et al. PRUNE2 is a human. prostate cancer suppressor. regulated by the intronic long noncoding RNA PCA3. Proc Natl. Acad Sci. U S A. 2015;112(27):8403–8.
7. Lee YS, Dutta A. MicroRNAs in cancer. Annu Rev Pathol. 2009;4:199–227.
8. Rupaimoole R, Slack FJ. MicroRNA therapeutics: towards a new era for the management of cancer and other diseases. Nat Rev Drug Discov. 2017;16(3):203–22.
9. He JH, Han ZP, Zou MX, Wang L, Lv YB, Zhou JB, Cao MR, Li YG. Analyzing the LncRNA, miRNA, and mRNA Regulatory Network in Prostate Cancer with Bioinformatics Software. J Comput Biol. 2018;25(2):146–57.
10. Shao M, Yu Z, Zou J. LncRNA-SNHG16 Silencing Inhibits Prostate Carcinoma Cell Growth, Downregulate GLUT1 Expression, and Reduce Glucose Uptake. Cancer Manag Res. 2020;12:1751–7.
11. Zhu H, Zeng Y, Zhou CC, Ye W. SNHG16/miR-216-5p/ZEB1 signal pathway. contributes to the tumorigenesis of cervical cancer cells. Archives of biochemistry and. biophysics. 2018; 637: 1–8.
12. Zhong JH, Xiang X, Wang YY, Liu X, Qi LN, et al. The lncRNA SNHG16 affects. prognosis in hepatocellular. carcinoma by regulating p62 expression. J. J Cell Physiol. 2020.;235(2):1090–1102.
13. Zhao W, Fu H, Zhang S, Sun S, Liu Y. LncRNA SNHG16 drives proliferation,migration,. and invasion of hemangioma endothelial cell through modulation of miR-520d-3p/STAT3. axis. Cancer medicine. 2018; 7(7):3311–20.
14. Qiu X, Zhu J, Sun Y, Fan K, Yang DR, Li G, Yang G, Chang C. TR4 nuclear receptor increases prostate cancer invasion via decreasing the miR-373-3p expression to alter TGFβR2/p-Smad3 signals. Oncotarget. 2015;6(17):15397–409.
15. Zhu B, Kyprianou N. Transforming growth factor beta and prostate cancer. Cancer Treat Res. 2005;126:157–73.
16. Maruyama T, Nishihara K, Umikawa M, Arasaki A, Nakasone T, Nimura F, et al. MicroRNA-196a-5p is a potential prognostic marker of delayed lymph node metastasis in early-stage tongue squamous cell carcinoma. Oncol Lett. 2018;15(2):2349–63.
17. Prensner JR, Iyer MK, Sahu A, Asangani IA, Cao Q, et al. The long noncoding RNA. SChLAP1 promotes. aggressive prostate cancer and antagonizes the SWI/SNF complex. Nature genetics. 2013; 45(11): 1392–1398.

18. Yu M, Ohira M, Li Y, Niizuma H, Oo ML, et al. High expression of ncRAN, a novel. non-coding. RNA mapped to chromosome 17q25.1 is associated with poor prognosis in. neuroblastoma. Int J Oncol. 2009;34(4):931–8.
19. Lian D, Amin B, Du D, Yan W. Enhanced expression of the long non-coding RNA SNHG16 contributes to gastric cancer progression and metastasis. Cancer biomarkers. 2017;21(1):151–60.
20. Xu F, Zha G, Wu Y, Cai W, Ao J. Overexpressing lncRNA SNHG16 inhibited HCC proliferation and chemoresistance by functionally sponging hsa-miR-93. OncoTargets therapy. 2018;11:8855–63.
21. Leeman JE, Chen MH, Huland H, Graefen M, D'Amico AV, Tilki D. Advancing Age and the Odds of Upgrading and Upstaging at Radical Prostatectomy in Men with Gleason Score 6 Prostate Cancer. Clin Genitourin Cancer. 2019;17(6):e1116–21.
22. Bernard B, Burnett C, Sweeney CJ, Rider JR, Sridhar SS. Impact of age at diagnosis of de novo metastatic prostate cancer on survival. Cancer. 2020;126(5):986–93.
23. Bai S, Cao S, Jin L, Kobelski M, Schouest B, Wang X, Ungerleider N, et al. A positive role of c-Myc in regulating androgen receptor and its splice variants in prostate cancer. Oncogene. 2019;38(25):4977–89.
24. Waghray A, Schober M, Feroze F, Yao F, Virgin J, Chen YQ. Identification of differentially expressed genes by serial analysis of gene expression in human prostate cancer. Cancer Res. 2001;61(10):4283–6.
25. DuPree EL, Mazumder S, Almasan A. Genotoxic stress induces expression of E2F4, leading to its association with p130 in prostate carcinoma cells. Cancer Res. 2004;64(13):4390–3.
26. Majumder S, Bhowal A, Basu S, Mukherjee P, Chatterji U, Sengupta S. Deregulated. E2F5/p38/SMAD3 Circuitry Reinforces the Pro-Tumorigenic Switch of TGFβ Signaling in. Prostate Cancer. J Cell Physiol. 2016;231(11):2482–92.
27. Xu W, Zeng F, Li S, Li G, Lai X, Wang QJ, Deng F. Crosstalk of protein kinase C ε with. Smad2/3. promotes tumor cell proliferation in prostate cancer cells by enhancing aerobic. glycolysis. Cell Mol Life Sci. 2018;75(24):4583–98.
28. Yang F, Strand DW, Rowley DR. Fibroblast growth factor-2 mediates transforming growth factor-beta action in prostate cancer reactive stroma. Oncogene. 2008;27(4):450–9.
29. Lv J, Fan HX, Zhao XP, Lv P, Fan JY, et al. Long non-coding RNA Unigene56159 promotes epithelial-mesenchymal transition by acting as a ceRNA of miR-140-5p in hepatocellular carcinoma cells. Cancer letters. 2016;382(2):166–75.
30. Keklikoglou I, Koerner C, Schmidt C, Zhang JD, Heckmann D, et al. MicroRNA-520/373 family functions as a tumor suppressor in estrogen receptor negative. breast cancer by. targeting NF-κB and TGF-β signaling pathways. Oncogene. 2012;31(37):4150-63.
31. Nakata K, Ohuchida K, Mizumoto K, Aishima S, Oda Y, et al. Micro RNA-373 is down-regulated in pancreatic cancer and inhibits cancer cell invasion. Ann Surg Oncol. 2014;21(Suppl 4):564-74.
32. Voorhoeve PM, le Sage C, Schrier M, Gillis AJ, Stoop H, et al. A genetic screen implicates miRNA-372 and miRNA-373 as oncogenes in testicular germ cell tumors. Cell. 2006;124(6):1169–81.

33. Nadauld LD, Garcia S, Natsoulis G, Bell JM, Miotke L, et al. Metastatic tumor evolution. and organoid modeling implicate TGFBR2 as a cancer driver in diffuse gastric cancer. Genome biology. 2014; 15(8):428.
34. Moon H, Ju HL, Chung SI, Cho KJ, Eun JW, et al. Transforming Growth Factor-beta. Promotes Liver. Tumorigenesis in Mice via Up-regulation of Snail. Gastroenterology. 2017.;153(5): 1378–1391.
35. Qin T, Barron L, Xia L, Huang H, Villarreal MM, Zwaagstra J, Collins C, et al. A novel highly potent trivalent TGF-β receptor trap inhibits early-stage tumorigenesis and tumor cell invasion in murine Pten-deficient prostate glands. Oncotarget. 2016;7(52):86087–102.

Tables

Table 1
Patient clinical characteristics (n = 80).

Factors	Statistics
Age (years)	54.88 ± 10.35
Gleason score	6 (5–8)
TNM stage	2 (1–3)
sPSA at enter (ng/mL)	48.08 ± 21.31
< 20 ng/mL	11 (13.75%)
≥ 20 ng/mL	69 (86.25%)
SNHG16	3.21 (2.68–3.96)
hsa-miR-373-3p	0.40 (0.21–1.05)
TGFβR2	2.22 (1.47–3.10)
Abbreviations: TNM,Tumor Node Metastasis; sPSA, serum prostate-specific antigen. Data are presented as mean ± standard deviation, median with interquartile interval [Q1-Q3] (%), and the number and percentage.	

Table 2
The correlation with patient's characteristics and SNHG16, hsa-miR-373-3p and TGFBR2 expression (n = 80).

Factors	Cases (n)	SNHG16 expression		*P* value	miR-373-3p expression		*P* value	TGFβR2 expression		*P* value
		Low(n)	High (n)		Low (n)	High (n)		Low (n)	High (n)	
Age (years)										
< 60	55	21	34	0.007	39	16	0.789	16	39	0.606
≥ 60	25	2	23		19	6		9	16	
Gleason score										
< 7	41	15	26	0.141	25	16	0.024	17	24	0.055
> 7	39	8	31		33	6		8	31	
TNM stage										
T1	33	11	22	1.000	22	11	0.598	8	25	1.000
T2	20	7	13		15	5		9	11	
T3/T4	27	5	22		21	6		8	19	

Abbreviations: TNM,Tumor Node Metastasis. Data are presented as the number. Fisher's exact test was used to descriptive analysis by the IBM SPSS Statistics 20.0 software, two-side. $P < 0.05$ was considered to suggest a significant difference.

Figures

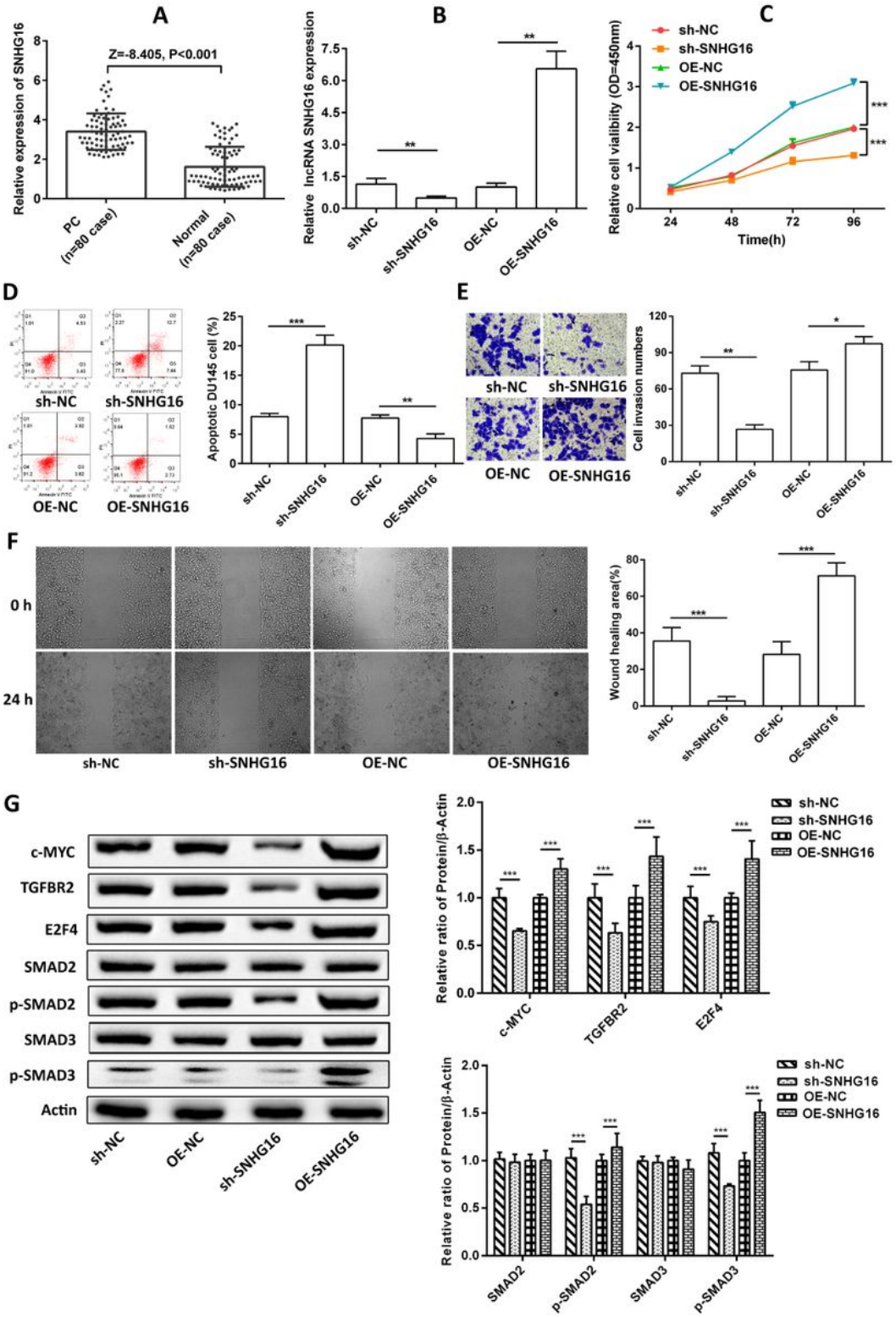

Figure 1

SNHG16 promoted tumor cell proliferation, migration and invasion by regulating TGFBR2/SMAD signaling. The expression of SNHG16 in PCa tissues were detected by qPCR (A). The expression of SNHG16 was assayed after knockdown and overexpression SNHG16 by qPCR (B). Overexpression or knockdown of SNHG16 influenced the DU-145 cell viability (C), apoptosis (D), invasion (E), and migration (F). The protein expression levels of c-MYC, TGFBR2, E2F4, SMAD2, p-SMAD2, SMAD3, and p-SMAD3

were determined by Western blot (G). Data were presented as mean ±standard deviation. All cell-related experiments were repeated three times. *P < 0.05, **P < 0.01, and ***P < 0.001. Mann–Whitney U test (A) and one-way ANOVA analysis with LSD post-hoc test were used, two-sided.

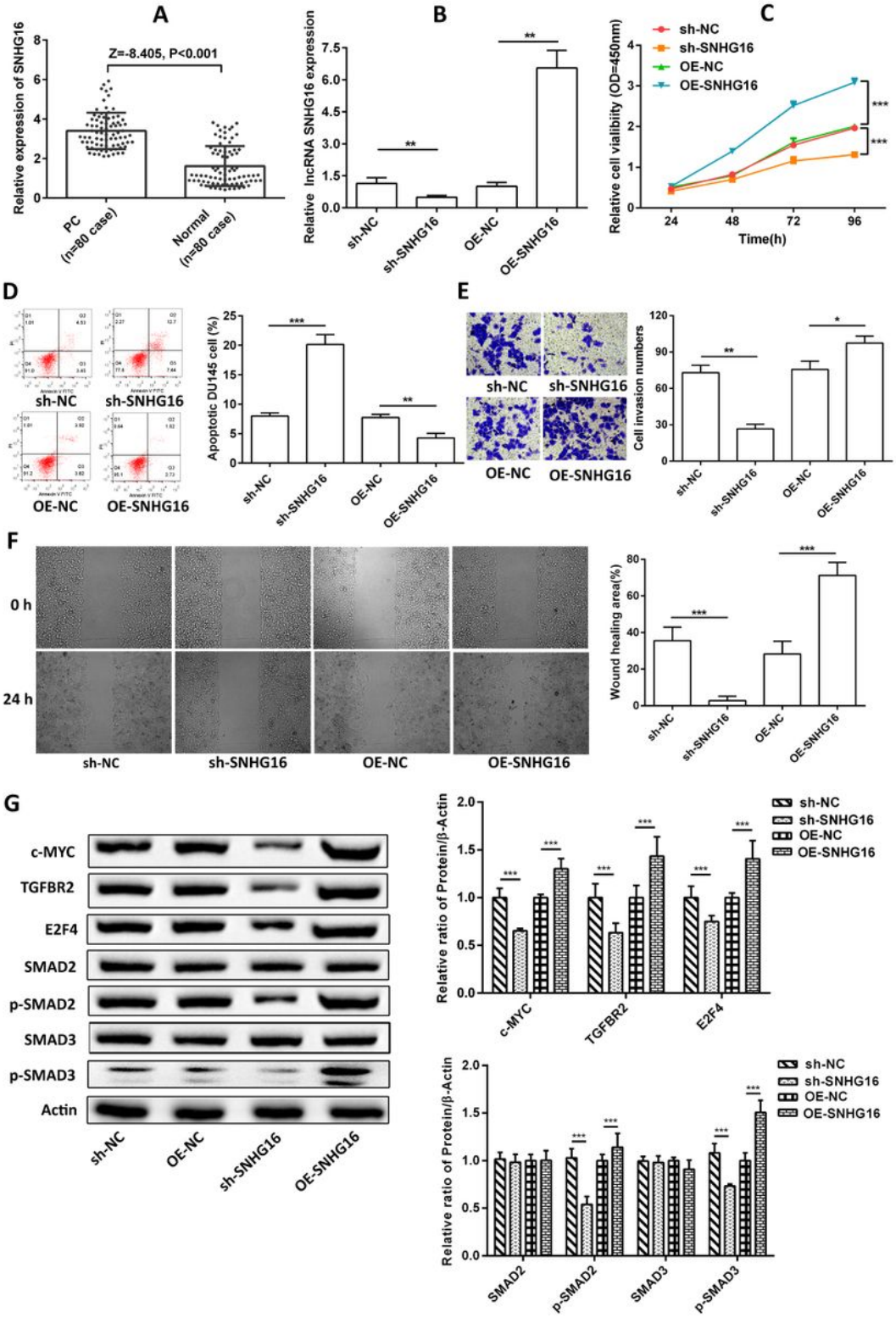

Figure 1

SNHG16 promoted tumor cell proliferation, migration and invasion by regulating TGFBR2/SMAD signaling. The expression of SNHG16 in PCa tissues were detected by qPCR (A). The expression of

SNHG16 was assayed after knockdown and overexpression SNHG16 by qPCR (B). Overexpression or knockdown of SNHG16 influenced the DU-145 cell viability (C), apoptosis (D), invasion (E), and migration (F). The protein expression levels of c-MYC, TGFBR2, E2F4, SMAD2, p-SMAD2, SMAD3, and p-SMAD3 were determined by Western blot (G). Data were presented as mean ±standard deviation. All cell-related experiments were repeated three times. *P < 0.05, **P < 0.01, and ***P < 0.001. Mann–Whitney U test (A) and one-way ANOVA analysis with LSD post-hoc test were used, two-sided.

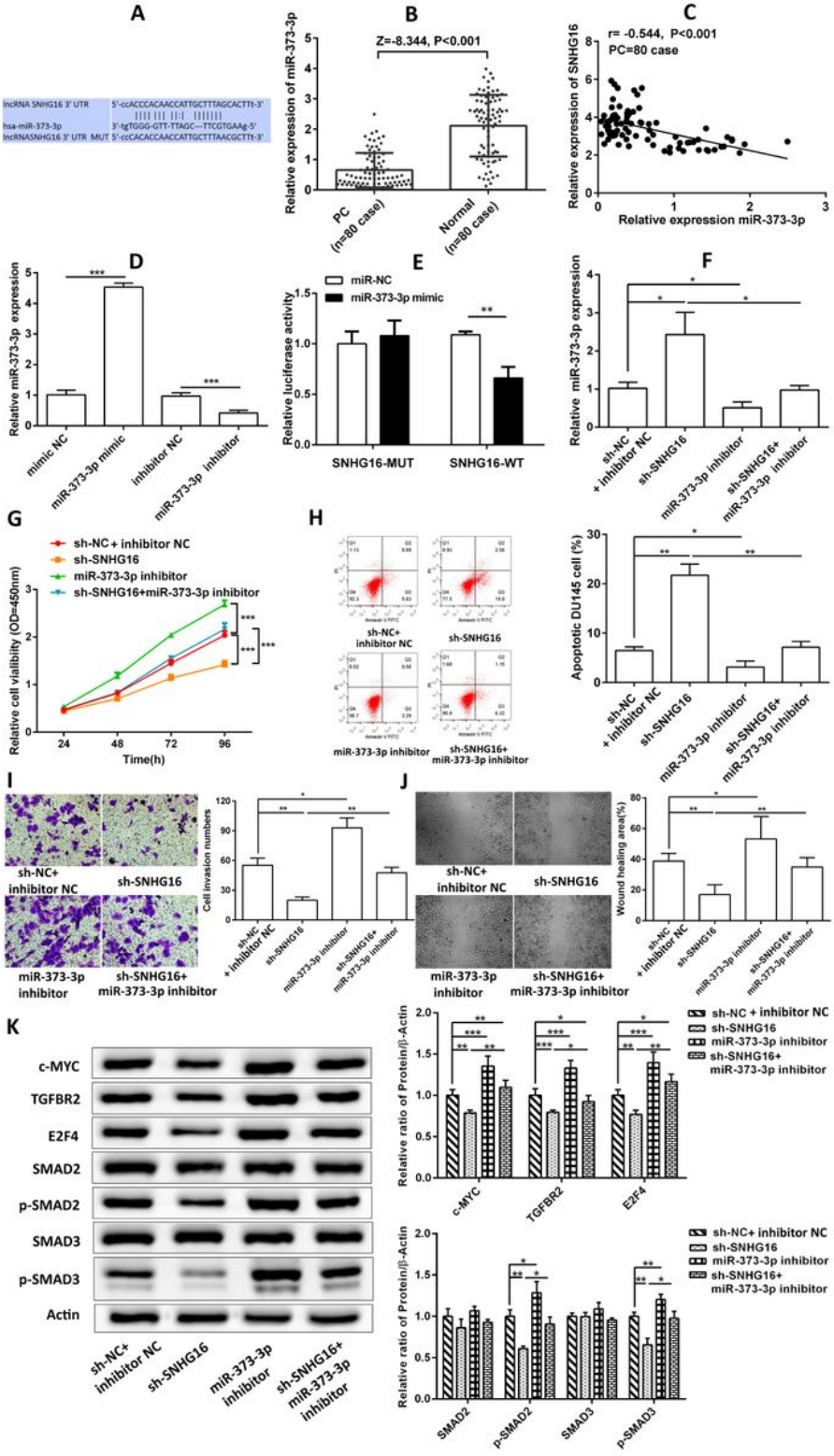

Figure 2

SNHG16 acts as miR-373-3p sponge to affect DU-145 cell biological processes via regulating TGFBR2/SMAD signaling. The target points of SNHG16 and hsa-miR-373-3p (A). The expression of hsa-miR-373-3p in PCa tissues were detected by qPCR (B). The Spearman correlation analysis was used between SNHG16 and hsa-miR-373-3p (C). The expression of hsa-miR-373-3p was assayed after transfecting hsa-miR-373-3p mimic and inhibitor by qPCR (D). The bioinformatical prediction of hsa-miR-373-3p and SNHG16 was verified by dual-luciferase assays system (E). Hsa-miR-373-3p inhibitor partially reversed the facilitation of SNHG16 depletion on hsa-miR-373-3p expression (F). Hsa-miR-373-3p inhibitor partially reversed the role of SNHG16 in viability (G), apoptosis (H), invasion (I), and migration (J) of DU-145 cell. The protein expression levels of c-MYC, TGFBR2, E2F4, SMAD2, p-SMAD2, SMAD3, and p-SMAD3 were determined by Western blot (G). Data were presented as mean ±standard deviation. All cell-related experiments were repeated three times. *P < 0.05, **P < 0.01, and ***P < 0.001. Mann–Whitney U test (B) and one-way ANOVA analysis with LSD post-hoc test were used, two-sided.

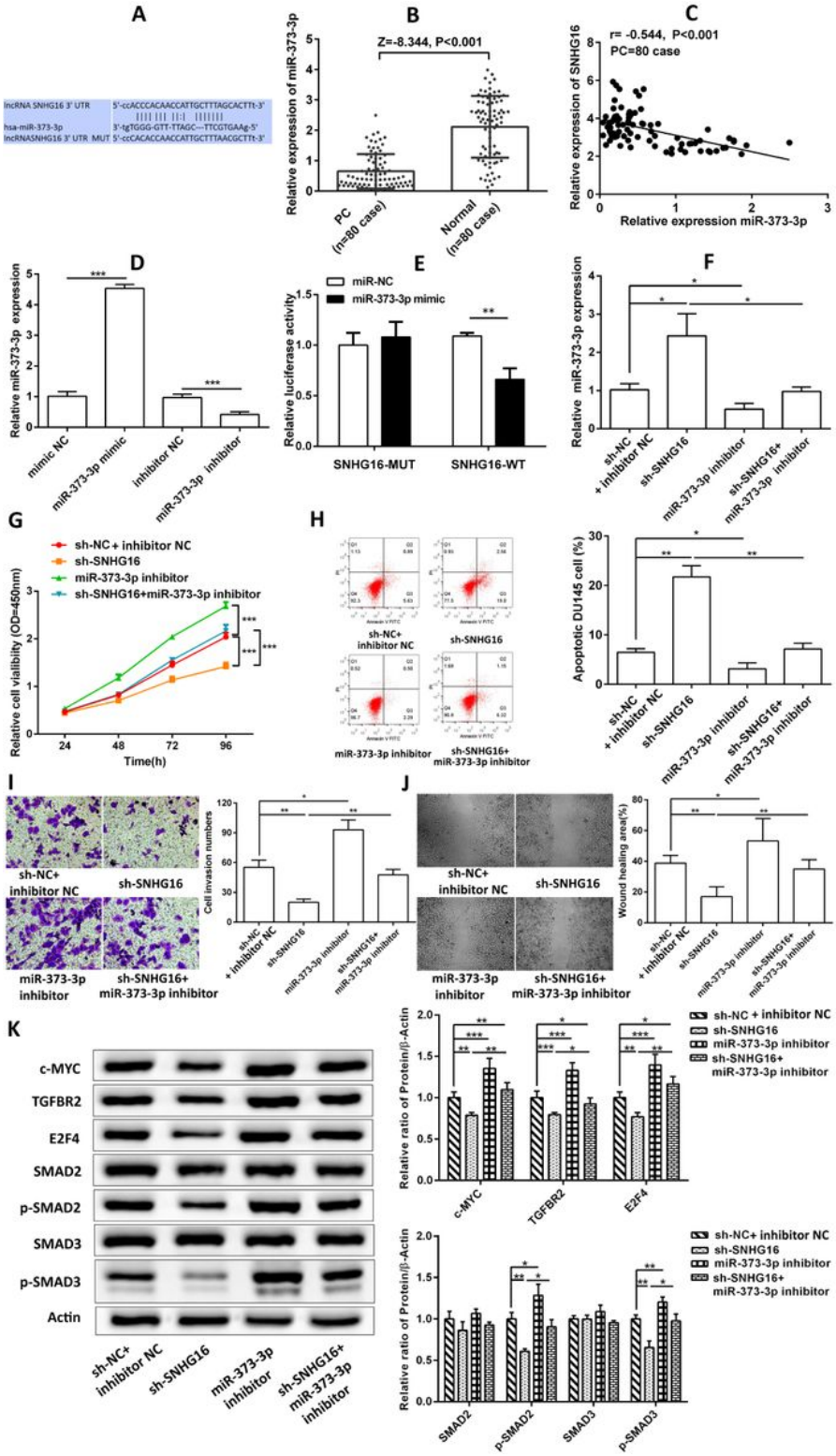

Figure 2

SNHG16 acts as miR-373-3p sponge to affect DU-145 cell biological processes via regulating TGFBR2/SMAD signaling. The target points of SNHG16 and hsa-miR-373-3p (A). The expression of hsa-miR-373-3p in PCa tissues were detected by qPCR (B). The Spearman correlation analysis was used between SNHG16 and hsa-miR-373-3p (C). The expression of hsa-miR-373-3p was assayed after transfecting hsa-miR-373-3p mimic and inhibitor by qPCR (D). The bioinformatical prediction of hsa-miR-

373-3p and SNHG16 was verified by dual-luciferase assays system (E). Hsa-miR-373-3p inhibitor partially reversed the facilitation of SNHG16 depletion on hsa-miR-373-3p expression (F). Hsa-miR-373-3p inhibitor partially reversed the role of SNHG16 in viability (G), apoptosis (H), invasion (I), and migration (J) of DU-145 cell. The protein expression levels of c-MYC, TGFBR2, E2F4, SMAD2, p-SMAD2, SMAD3, and p-SMAD3 were determined by Western blot (G). Data were presented as mean ±standard deviation. All cell-related experiments were repeated three times. *P < 0.05, **P < 0.01, and ***P < 0.001. Mann–Whitney U test (B) and one-way ANOVA analysis with LSD post-hoc test were used, two-sided.

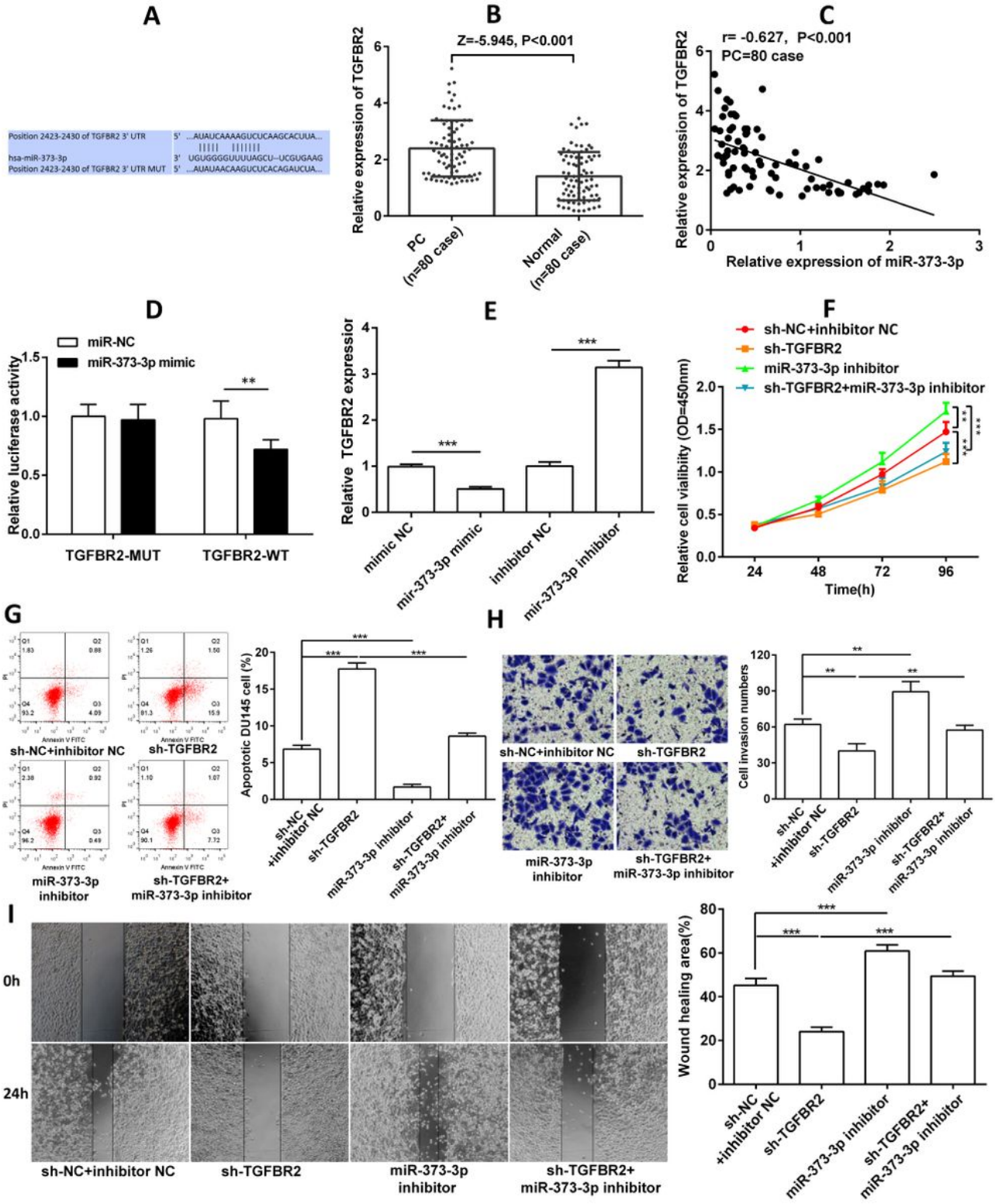

Figure 3

Hsa-miR-373-3p target TGFBR2 to mediate DU-145 cell biological processes. The target points of hsa-miR-373-3p and TGFBR2 (A). The expression of TGFBR2 in PCa tissues were detected by qPCR (B). The Spearman correlation analysis was used between TGFBR2 and hsa-miR-373-3p (C). The bioinformatical prediction of TGFBR2 and hsa-miR-373-3p was verified by dual-luciferase assays system (D). The expression of TGFBR2 was assayed after knockdown and overexpression TGFBR2 by qPCR (E). Knockdown of TGFBR2 partially reversed the role of hsa-miR-373-3p inhibitor on viability (F), apoptosis (G), invasion (H), and migration (I) of DU-145 cell. Data were presented as mean ±standard deviation. All cell-related experiments were repeated three times. **P < 0.01, and ***P < 0.001. Mann–Whitney U test (B) and one-way ANOVA analysis with LSD post-hoc test were used, two-sided.

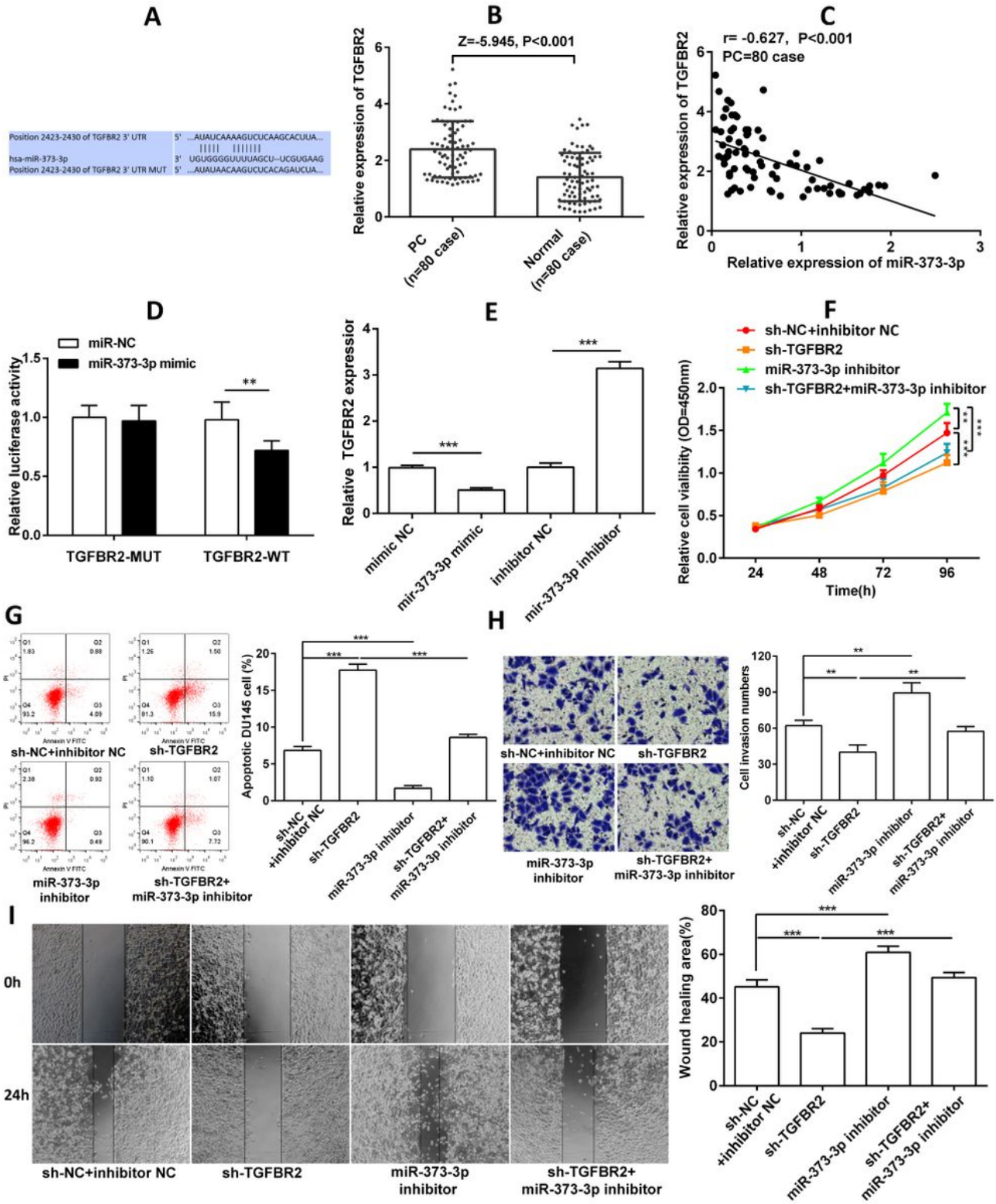

Figure 3

Hsa-miR-373-3p target TGFBR2 to mediate DU-145 cell biological processes. The target points of hsa-miR-373-3p and TGFBR2 (A). The expression of TGFBR2 in PCa tissues were detected by qPCR (B). The Spearman correlation analysis was used between TGFBR2 and hsa-miR-373-3p (C). The bioinformatical prediction of TGFBR2 and hsa-miR-373-3p was verified by dual-luciferase assays system (D). The expression of TGFBR2 was assayed after knockdown and overexpression TGFBR2 by qPCR (E).

Knockdown of TGFBR2 partially reversed the role of hsa-miR-373-3p inhibitor on viability (F), apoptosis (G), invasion (H), and migration (I) of DU-145 cell. Data were presented as mean ±standard deviation. All cell-related experiments were repeated three times. **P < 0.01, and ***P < 0.001. Mann–Whitney U test (B) and one-way ANOVA analysis with LSD post-hoc test were used, two-sided.